

VALIDATION OF DISPERSION MODELS FOR HIGH PRESSURE CARBON DIOXIDE RELEASES†

C.M. Dixon[1], S.E. Gant[2], C. Obiorah[3], and M. Bilio[4]
[1] Shell Global Solutions (UK), Shell Technology Centre Thornton, PO Box 1, Chester, CH1 3SH
[2] Health & Safety Laboratory, Harpur Hill, Buxton, SK17 9JN
[3] Shell Global Solutions International, Kessler Park 1, 2288GS Rijswijk, Netherlands
[4] Health & Safety Executive, Redgrave Court, Merton Road, Bootle, L20 7HS

Predictions from an integral model and two Computational Fluid Dynamics (CFD) models are compared to experimental data for confined and unconfined jet releases of dense phase carbon dioxide (CO_2). The releases studied are relevant in scale to leaks from above-ground pipes or vessels. For the unconfined cases, the jets consist of a horizontal discharge through either a $\frac{1}{2}''$ or $1''$ orifice, with the dense-phase CO_2 reservoir maintained at approximately 150 bar and close to ambient temperature. The confined release involves a $\frac{1}{2}''$ diameter jet discharging into a largely-enclosed steel container of dimensions $6 \times 2 \times 2$ metres. Measurements of temperature and concentration in the dispersing CO_2 plumes were obtained for these tests from experiments commissioned by Shell at the GL Spadeadam facility.

The integral model used is Shell FRED, which adopts a semi-empirical jet model for the momentum-dominated part of the release and a similarity model for the subsequent dense gas dispersion, if required. FRED assumes Homogeneous Equilibrium (HE) between the CO_2 particles and the vapour phase, i.e. the particles and surrounding vapour share the same temperature and velocity. Since FRED was primarily designed for hydrocarbon hazards it does not actually consider solid particles but, rather, the liquid-vapour line is extrapolated down to atmospheric pressure and the particles are treated as liquid; the effect of this approximation is discussed.

Two different CFD dispersion models are tested: the first has been developed in the OpenFOAM CFD software and assumes HE, whilst the second has been developed in Ansys-CFX and uses a particle-tracking approach to simulate the sublimating solid CO_2 particles. Both FRED and the two CFD models account for the latent heat effects associated with humidity and the condensation of water vapour in the cold CO_2 cloud.

The results from the model comparisons are used to assess the suitability of fast consequence models like FRED to simulate unconfined jet releases of dense phase CO_2. The findings provide useful information for the assessment of potential hazards presented by Carbon Capture and Storage (CCS) infrastructure.

1. INTRODUCTION

A number of industrial-scale Carbon Capture and Storage (CCS) projects are currently being planned in the UK[1] including the Don Valley Power Project[2] in Yorkshire, and the Peterhead power station[3] in Aberdeenshire. In total, there are nine UK CCS projects that have applied for EU funding from the New Entrant Reserve (NER) scheme[4]. In many of these projects, carbon dioxide (CO_2) will be transported or stored in its liquid state, i.e. at a pressure above 74 bar and temperature below 31ºC. As part of the design and risk assessment process for the CCS infrastructure, an understanding is required of the consequences of an intentional or accidental release of liquid CO_2. The relevant CCS infrastructure will include compressor stations, pipelines transporting the CO_2 from the power station to the reservoir injection site and, in some cases, equipment on offshore platforms.

The focus of the present work is on the validation of CO_2 release models against experimental data. For the purposes of model validation, predictions are compared to measurements from a programme of CO_2 release experiments commissioned by Shell at the GL Spadeadam test site in Cumbria in late 2010. These experiments consisted of steady-state horizontal discharges onto an open test pad with a well-defined mass flow rate of liquid CO_2. The pad was well instrumented to provide measurements of temperature and gaseous CO_2 concentration at numerous locations, for distances up to around 80 m from the release orifice. In addition, a more limited set of tests was conducted in which liquid CO_2 was discharged into a largely-enclosed steel container of dimensions $6 \times 2 \times 2$ metres.

[1]http://www.ccsassociation.org/why-ccs/ccs-projects/current-projects (accessed May 2012)
[2]http://www.2coenergy.com/don_valley_power_project.html (accessed May 2012)
[3]http://www.sse.com/EnergyPolicy/FutureEnergyNeeds/Generation/CCS/ (accessed May 2012)
[4]http://www.decc.gov.uk/en/content/cms/news/pn11_013/pn11_013.aspx (accessed May 2012)

The results from various models are compared to the measured concentrations and temperatures to assess the strengths and weakness of different underlying model assumptions, and the degree of error in model predictions. The findings will prove to be useful for the assessment of potential hazards presented by CCS infrastructure.

2. REVIEW OF PREVIOUS STUDIES

There have been a number of recent publications examining the release and dispersion of CO_2. In the earlier of the two papers published by MMI Engineering (Dixon and Hasson, 2007), dispersion simulations were performed using the ANSYS-CFX Computational Fluid Dynamics (CFD) code. Solid CO_2 particles were not included explicitly in the model but were instead simulated using a scalar representing the particle concentration. This approach was taken to avoid the additional computing time associated with Lagrangian particle tracking. However, one of its limitations was that in calculating the heat and mass exchange between the particles and the gas phase, it was necessary to assume a constant particle diameter. The distribution of the source of CO_2 gas resulting from particle sublimation may have therefore been poorly predicted, since the rate of sublimation increases as the particle size decreases in the jet. In addition, the particle temperature was assumed to remain constant at the sublimation temperature of −78ºC i.e. a "boiling" assumption was made.

In the second MMI paper (Dixon *et al.*, 2009), the particles were modelled using a Lagrangian particle tracking approach. However, particles were still assumed to remain at a constant temperature of −78ºC. It is discussed later, in Section 4, that in reality the particle temperature is expected to fall in the jet, to perhaps as low as −100ºC. In both of the MMI studies, the release rate was calculated using a Homogenous Equilibrium Model (HEM) rather than the Bernoulli equation which has been used in the present paper. The method used to model the expansion of CO_2 from the orifice to the atmospheric pressure was, however, essentially the same as that described later in this paper.

The UK Health and Safety Executive (HSE) have published a number of papers on CO_2 release and dispersion modelling. In the first of these, Shuter *et al.* (2010) provided a review of CCS safety issues from the perspective of the UK HSE. Modelling was not considered in detail, but source term modelling was included under the heading of "knowledge gaps" where it was stated that hazard ranges are sensitive to the source term model assumptions. McGillivray *et al.* (2009) compared the risks from CO_2 pipelines and natural gas pipelines. PHAST was used to calculate the CO_2 gas dispersion and HSE in-house tools were used to compare the risks. Only gaseous inventories were considered and two hole sizes were modelled in addition to full-bore ruptures. Interestingly, some analysis was included of the deflection of the jet angle due to its impact on the crater walls. Overall, the hazard due to a CO_2 pipeline in the pressure range considered was found to be similar to a corresponding natural gas pipeline. Harper (2010) carried out a number of modelling exercises for CO_2 dispersion using the DRIFT model and two versions of PHAST. The paper was mostly concerned with releases due to catastrophic vessel failures that lead to large instantaneous releases, rather than the jet releases that are considered in the present paper.

Webber (2011) presented a methodology for extending existing two-phase homogeneous equilibrium integral models for flashing jets to the three-phase case for CO_2. As the flow expands from the reservoir conditions to atmospheric pressure, it was assumed that the pressure, temperature, density and the jet cross-sectional area would vary continuously through the triple point, whilst the mass and momentum would be conserved. This led to the conclusion that there must be a discontinuity in the enthalpy and CO_2 liquid fraction, in a similar manner to the energy loss associated with flow passing through a hydraulic jump. The paper only considered theoretical model development and did not show any comparisons to data.

Gant and Kelsey (2012) examined the effect of concentration fluctuations in gaseous releases of CO_2. The Toxic Load (TL)[5] is proportional to concentration to the power eight for CO_2 and therefore it increases rapidly if there are any concentration fluctuations in the plume. To examine the significance of this effect, the TL in jets of gaseous CO_2 was examined using three different models: a quasi-empirical Probability Density Function (PDF) model that accounted for concentration fluctuations, a model based solely on the mean concentration with no fluctuations, and a third model which assumed that the concentration fluctuated with an assumed square wave variation over time. The Specified Level of Toxicity (SLOT) and Significant Likelihood of Death (SLOD) hazard distances were shown to be under-predicted if the effects of concentration fluctuations were ignored. It was also demonstrated that the assumed square-wave fluctuation model provided conservative predictions of the distances from the CO_2 source to the SLOT and SLOD.

DNV Software has produced two key papers on CO_2 release and dispersion modelling. In the first, Witlox *et al.* (2009) described an extension to the existing model in PHAST version 6.53.1 to account for the effects of solid CO_2. The modifications consisted principally of changing the way in which equilibrium conditions were calculated in the expansion of CO_2 to atmospheric pressure, to ensure that below the triple point, conditions followed the sublimation curve in the phase diagram, rather than extrapolating the evaporation curve. Although the revised model was validated against experimental data, the measurements were confidential and could not be reported. In the second of the papers (Witlox *et al.*, 2011), the results of sensitivity tests were reported for both liquid and supercritical CO_2 releases from vessels and pipes with the revised PHAST version 6.6 model. Again, no experimental validation was presented due to data confidentiality.

E.ON have published a number of studies in support of their proposed CCS programme (Mazzoldi *et al.*,

[5]http://www.hse.gov.uk/chemicals/haztox.htm (accessed August 2012)

2008a, 2008b, 2011; Hill *et al.*, 2011). The most relevant publications to the present work are by Mazzoldi *et al.* (2011) and Hill *et al.* (2011), which considered atmospheric dispersion from pipeline and vessel releases. The former paper compared simulations from the heavy gas model ALOHA to the CFD model Fluidyn-Panache. Although the work focused on discharges of dense-phase CO_2 from a 100 bar release, only the gaseous stage of the discharges were modelled. The bulk of the analysis consisted of comparisons between the two models, rather than experimental data. Some sample data from an earlier study of the Kit Fox trials (Mazzoldi *et al.*, 2008a) was included in the paper, where the same models were compared to experimental data at one measurement location, which showed that ALOHA over-predicted the gas concentration. It was concluded from this that "Gaussian/dense-gas simulations can over-estimate the risk in a way that would prejudice the widespread introduction of the technology". However, a more complete analysis of the ALOHA and Panache model predictions against multiple Kit Fox trial measurements in their previous work showed that both models under-predicted concentrations on average.

Hill *et al.* (2011) presented CFD and PHAST simulations of dense-phase CO_2 releases from a 0.5 m diameter hole in a pipeline, located at an elevation of 5 m above flat ground. Rather than model the time-varying depressurization of the pipeline, steady-state flow rates were calculated at the orifice assuming saturated conditions. The method described by Fauske and Epstein (1988) was used to calculate the source conditions once the two-phase jet had expanded to atmospheric pressure. CFD simulations were performed using the ANSYS-CFX code with a Lagrangian particle-tracking model for the solid CO_2 particles. To examine the effect of the particle size, three size distributions were tested: from 10 to 50 μm, from 50 to 100 μm and from 50 to 150 μm. Simulations were also performed with no solid CO_2 particles. The results showed that sublimation of the particles led to cooling of the CO_2 plume, which affected its dispersion behaviour, although the results were relatively insensitive to the particle size. Predicted gas concentrations downwind from the release were somewhat lower using PHAST version 6.6 as compared to the CFD results but there was no comparison of model predictions to experiments.

One of the differences between the CFX model used by Hill *et al.* (2011) and that used in the present study is that it appears that their Lagrangian model did not account for the effects of turbulence on the dispersion of the solid CO_2 particles. The particle tracks were not spread throughout the plume but instead followed closely the plume centreline. Ignoring turbulent dispersion effects can have a significant influence on the model predictions, particularly the temperature. Turbulence has the effect of bringing particles into contact with parts of the jet at a higher temperature and lower CO_2 concentration. This tends to increase the rate of sublimation and increase the radius of the region cooled by the sublimating particles. In the present work, turbulent dispersion effects have been included in the CFX model, although this has required a greater number of particles to be simulated, with consequently longer computing times.

A second difference between the model used in the present work and that presented by Hill *et al.* (2011) is that it is assumed here that the solid CO_2 particles are much smaller (i.e. an initial particle diameter of 5 μm). This choice has been made based on analysis of CO_2 experiments, which showed that gas temperatures in the plume fell well below −78ºC. In addition, the particle size distribution model recently developed by Hulsbosch-Dam *et al.* (2012) suggested that the particle diameter would be around 5 μm for CO_2 releases at a pressure of 100 bar, when the difference between the CO_2 and ambient temperatures was around 80ºC. The effect of having smaller particles in the present model is likely to cause more rapid sublimation, which should produce a more significant reduction in gas temperature in the jet.

3. EXPERIMENTAL ARRANGEMENT

In the experiments conducted at GL Spadeadam, the CO_2 inventory was contained within a 24″ diameter vessel with a volume of 6.3 m^3. Two pipes were connected at opposite ends of this vessel. From one end, a length of pipework connected the vessel to an orifice which was located at a height of 1 m above the surface of the concrete test pad. The pipework connected to the orifice included a Coriolis flow meter which was used to measure directly the CO_2 mass flow rate. Orifice sizes up to 1″ were used in the tests, with releases directed horizontally.

At the opposite end of the vessel, a connection led to a pad gas line which was filled with liquid CO_2 at the same conditions as within the vessel. The inlet to the pad gas line was connected to a nitrogen reservoir at a constant supply pressure, which enabled steady-state CO_2 releases to be produced. The pad gas line was inclined from the horizontal to minimise the surface area between the nitrogen and liquid CO_2, and releases were stopped prior to nitrogen entering the test vessel, to prevent it from contaminating the CO_2. The temperature and pressure were measured at a number of locations within the vessel and the pipework, including one location immediately upstream of the orifice.

In addition to the instrumentation of the vessel and pipework, there was significant field instrumentation on the test pad. Temperature and oxygen depletion measurements were taken on arcs at 20, 40, 60 and 80 m from the release, together with centreline locations at 5, 10 and 15 m. The oxygen depletion measurements were used to infer CO_2 concentration. All of the measurement stands were fitted with temperature and concentration instruments at 1 m above pad level (i.e. at the same height as the orifice) and some stands featured additional instruments at heights of 0.3 m and 3 m above the pad. On the jet centreline there were additional temperature measurements at 1, 2, 3 and 4 m from the release and at other locations there were concentration measurements from sampling devices and commercial point CO_2 detectors in some of the tests.

Two anemometer masts were used to measure the atmospheric conditions. Both masts used sonic anemometers to record both wind speed and direction. Measurements from the mast positioned upwind from the release point were used to define the wind speeds in the dispersion simulations.

4. CALCULATION METHODS

The simulations were split into three consecutive stages: for the outflow, expansion and dispersion. In the first, outflow stage, the mass flow rate was calculated together with various properties at the release plane (i.e. the orifice). In the second, expansion stage, the process by which the liquid or liquid/vapour mixture at the orifice was transformed into a gas/solid mixture at atmospheric pressure was modelled. Finally, in the third stage, the dispersion of CO_2 downstream from the expansion zone was modelled, which required the physical processes associated with sublimation of solid CO_2 particles and condensation of water vapour in the jet to be taken into account. It should be noted that FRED does not consider solid particles but, rather, the liquid-vapour line is extrapolated down to atmospheric pressure and the particles are treated as evaporating liquid droplets.

Calculations were performed using three different models: FRED Pressurised Release (PR), OpenFOAM and ANSYS-CFX. The first of these, PR, is an integral model that forms part of the Shell FRED software package (Betteridge and Roy, 2010). It has been used to calculate all stages of the release, including the outflow, expansion and dispersion. The second and third models, OpenFOAM and ANSYS-CFX, are both CFD models that were used to calculate only the final stage dispersion process. Both PR and OpenFOAM assumed thermodynamic equilibrium whereas ANSYS-CFX used a Lagrangian particle-tracking approach.

4.1 THERMODYNAMIC EQUILIBRIUM

A brief discussion of the thermodynamic equilibrium concept is provided here since it forms a key part of the PR and OpenFOAM models. The starting point for the discussion corresponds to a position at the end of the expansion zone in a jet of pure CO_2, which contains both vapour and solid CO_2 particles at the sublimation temperature of -78ºC. As air is added into such a mixture, the CO_2 gas concentration starts to decrease so that the vapour pressure exerted by the solid CO_2 particles exceeds the CO_2 partial pressure in the surrounding gas mixture. The solid therefore starts to sublime and its temperature falls in order to supply the heat of sublimation. There is an exchange of heat from the warmer gas mixture to the cold particles so that the temperature of both the gas and solid phases decreases. If the particles are sufficiently small, this transfer of heat occurs rapidly, i.e. the solid and gas phases share essentially the same temperature. The solid CO_2 continues to sublime and the temperature of the solid-gas mixture falls to a point where eventually the saturation vapour pressure at the particle surface matches the partial pressure of CO_2 in the gas mixture. At this point, no further sublimation takes place and equilibrium conditions are established. Moving further downstream in the jet, this process occurs continuously, with further air entrainment producing lower temperatures. The resulting behaviour is such that the temperature follows the saturation curve for solid-vapour equilibrium in the pressure-temperature phase diagram as the distance from the orifice increases (where the pressure in the phase diagram refers to the partial pressure of CO_2 rather than the atmospheric pressure). This process continues up to the point where all of the solid CO_2 has sublimated. Further entrainment into the jet beyond this point causes the temperature to increase, as the cold CO_2-air mixture mixes with warmer ambient air.

A second application of the thermodynamic equilibrium analysis relates to interpretation of the experiments. Analysis of the measurement data from the experiments showed that the oxygen depletion sensors (which relied upon a chemical reaction to measure the oxygen concentration) were adversely affected by the very low temperatures in the jet and produced unreliable measurements at later times in a release. Since the solid CO_2 particles were expected to be very small (Hulsbosch-Dam *et al.*, 2012), it was considered reasonable to assume thermodynamic equilibrium in the jet. By making this assumption, the total CO_2 concentration and the gas temperature could be directly related. This approach is explained by Witlox *et al.* (2009) and it will not be repeated here, but in this way CO_2 concentrations have been inferred from temperature measurements, which are presented in later sections. It should be noted that the results of this analysis are sensitive to the initial solid fraction of CO_2, which was not measured directly in the experiments, and this introduces a degree of uncertainty into the inferred concentration data.

4.2 OUTFLOW MODEL

The mass flow rate of CO_2 from the orifice was calculated using the Bernoulli equation. Use of the Bernoulli equation is based on the assumption of a meta-stable liquid at the orifice due to the residence time of the fluid through the orifice being too short for nucleation of vapour bubbles. The Bernoulli equation results in the well-known formula for the mass flux, G:

$$G = C_d A \sqrt{2\rho(P_0 - P_{atm})} \quad (1)$$

where C_d is the discharge coefficient, A the orifice area, ρ the fluid density, P_0 the stagnation pressure and P_{atm} the atmospheric pressure. A value of 0.6 was assumed for C_d in the present work, which accounts for the narrowing of the jet (i.e. the vena contracta) at the location where the pressure reaches atmospheric.

Comparison of the predicted mass flow rate to the measurements showed that Equation (1) slightly over-estimated the mass flow rate, giving a value up to around 10% greater than the measured values.

4.3 EXPANSION TO ATMOSPHERIC PRESSURE

The flashing process that takes place as the jet expands from the orifice to the atmospheric pressure was calculated using global conservation laws for mass, momentum and energy (Post, 1994; Harper, 2005). The inlet to the CFD calculations was taken to be at the end of the flashing depressurisation zone.

To calculate the post-flash conditions, it was assumed that there is a distinct depressurisation zone in which the fluid rapidly expands to atmospheric pressure and that a two-phase jet exists beyond this point. In the depressurisation zone it is assumed that there is no entrainment, and friction is neglected. A control volume is then constructed around the expansion zone, and equations are derived for the mass, energy and momentum conservation between the inlet and outlet of this volume. Assuming thermodynamic equilibrium then allows the source radius, velocity and solid fraction to be obtained. The orifice pressure is above atmospheric pressure so that the gas is accelerated in the expansion zone.

4.4 FRED DISPERSION MODEL

The Shell FRED (Fire Release Explosion Dispersion) software is composed of a suite of hazard modelling codes with a common interface. For the calculations presented here the Pressurised Release (PR) model is employed, which makes calls to a number of underlying codes. Following the flashing calculation, described in Section 4.3, the dispersion of CO_2 is calculated using a jet dispersion model, AEROPLUME, the results of which may then be passed on to the dense gas dispersion model HEGADAS. These models have been described in detail elsewhere (Post, 1994). An important aspect of the code to note in the present context is that it is assumed that a homogenous equilibrium exists between the particles and the air, i.e. the velocity, temperature and pressure of the two phases are assumed to be equal.

In the present work, the thermodynamics library employed by FRED did not account for solid CO_2, but instead the liquid-vapour saturation line was extrapolated to atmospheric pressure. Hence, following the flash process, FRED gave a gas/liquid mixture with liquid drops rather than solid particles. The subsequent gas plume consisted of a mixture of vapour and liquid CO_2, together with liquid and vapour water, and air.

4.5 OPENFOAM DISPERSION MODEL

In addition to the standard transport equations for mass, momentum, turbulence and energy, the OpenFOAM CFD model solved transport equations for two scalars, one to account for the mass fraction of pollutant (in this case CO_2) in the gas phase and another to track the mass concentration of solid (or liquid) pollutant. The gas-phase thermodynamic and transport properties were pre-calculated assuming thermodynamic equilibrium using a real gas equation-of-state and were presented to the solver as a set of lookup tables over temperature, pressure and pollutant mass fraction. Water vapour and liquid water were included in the gas phase using a homogenous equilibrium assumption so that the effects of condensation and evaporation were automatically captured. Only one set of momentum equations was solved since it was assumed that the solid CO_2, air and condensed water droplets shared the same velocity.

The density used by the solver was the gas density rather than the mixture density, and it did not include the contribution from the solid particles. The conservation equation for the transport of solid CO_2 was therefore expressed in terms of concentration (in kg/m^3), rather than a mass fraction, as follows:

$$\nabla \cdot \left(\boldsymbol{u}c - \nabla \frac{\mu_t}{St} c \right) = S_c \tag{2}$$

where c is the mass concentration of solid CO_2 in kg/m^3, $\boldsymbol{u}$ is the velocity vector, μ_t the turbulent viscosity, St the Schmidt number and S_c a source term due to particle sublimation. A source term of equal magnitude and opposite sign to S_c was included in the mass fraction equation. An additional term was also included in the enthalpy equation to account for the latent heat effects associated with sublimation, which was given by $S_h = -S_Y\, h_{sg}$, where h_{sg} is the latent heat of sublimation and S_Y the sublimation rate.

To determine the source terms S_c, S_Y and S_h it was assumed that thermodynamic equilibrium holds, i.e. that the solid particles and surrounding gas shared the same temperature. The equilibrium vapour pressure (which is a function of temperature) divided by the fluid pressure is then equal to the mole fraction of CO_2 in the vapour phase:

$$\frac{P_{eq}(T)}{P_{atm}} = m_{\mathrm{CO2}} \tag{3}$$

To enforce this condition, the following source terms were used, which reduced the solid concentration if the equilibrium vapour pressure exceeded the CO_2 mole fraction, until equilibrium was established:

$$S_C = -S_Y = -\beta(P_{eq} - m_{\mathrm{CO2}}\, P_{atm})Y \tag{4}$$

In the above equation, β is a constant that was chosen to be sufficiently large that the condition in Equation (3) was met, yet sufficiently small to retain numerical stability. The mass fraction, Y, was included in Equation (4) to ensure that the source term was zero if there was no solid CO_2 present. The equilibrium pressure, P_{eq}, was calculated from Antoine's equation.

Due to the presence of solid particles in the flow, small modifications were also necessary in the momentum equation. Turbulence was modelled using the standard $k-\varepsilon$ model.

The meshes employed in the OpenFOAM calculations were primarily hexahedral and were refined on geometrical surfaces and in specified regions, such as around the jet. In the present work, the source geometry

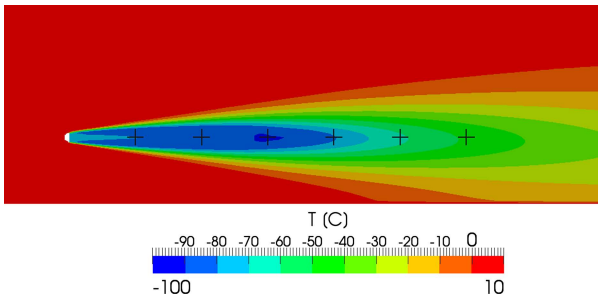

Figure 1. Gas temperature predicted by the OpenFOAM model for Test Case 3. Cross symbols are spaced at 1 m intervals along the jet axis

comprised a hemisphere representing the expanding "tulip", characteristic of the flashing zone, with a circular face for the jet inlet.

Sample results from the OpenFOAM model in the vicinity of the jet source are shown in Figure 1 for Test 3. Gas temperatures were predicted to fall from an initial value of −78ºC to reach a minimum of around −90ºC at a distance of around 2.5 m downstream from the source. Many of the solid CO_2 particles had sublimated completely by this distance. The maximum distance travelled by the particles was predicted to be around 3 m.

4.6 CFX DISPERSION MODEL

The CFX dispersion model was developed using a Lagrangian particle-tracking model in ANSYS-CFX version 13 (Ansys Inc, 2010). The process of sublimation was simulated using the standard droplet evaporation model as follows:

$$\frac{dm}{dt} = \min\left[\pi d \rho_g D_g Sh \frac{W_c}{W_g} \ln\left(\frac{1 - X_g}{\max\left[1 - X_c, \varepsilon_0\right]}\right), 0\right] \quad (5)$$

where dm/dt is the rate of mass loss from a particle, subscript c refers to the gas-phase CO_2 properties and g to the properties of the air-CO_2 gas mixture, W is the relative molecular mass, d the particle diameter, D the diffusivity, Sh the Sherwood number and ε_0 is a small number used here to avoid numerical difficulties when X_g becomes close to unity. The molar fractions, X_c and X_g, were calculated from:

$$X_c = \frac{\gamma_c \rho_g}{W_c C_g} \quad X_g = \frac{P_c^{sat}}{P} \quad (6)$$

where γ is the mass fraction, ρ the density, C the molar concentration ($C = P/R_u T$), P_c^{sat} the vapour pressure for the component evaporating, found from Antoine's equation, and P is the total pressure in the gas mixture.

At the CO_2 jet source in the CFX model, the solid particles were assigned an initial diameter of 5 μm, the same velocity as the surrounding CO_2 gas and a temperature equal to −78ºC. Unlike the approach taken in OpenFOAM, the CFX model allowed for slip between the gas and solid phases. The particle velocities were determined using the standard drag model of Schiller and Naumann (1933) combined with the stochastic dispersion model of Gosman and Ioannides (1981) to account for turbulence effects. The mass transfer from sublimation of the particles (Equation 5) produced a drop in the particle temperatures due to latent heat effects. The resulting temperature gradient between the gas and solid particles produced a transfer of heat, which was modelled using the Ranz-Marshall correlation (Ranz and Marshall, 1952).

In Lagrangian particle-tracking CFD simulations, the number of computational particles injected at the source is controlled independently of the mass flow rate or particle size. In the present simulations, 10,000 particles were released and tests were performed to ensure that increasing the number of particles had no effect on the results.

The way in which solid CO_2 particles interact with solid walls is subject to significant uncertainty and in the present simulations any particles impinging onto walls were assumed to rebound elastically and remain in the flow rather than to be deposited.

The modelled gas-phase consisted of a mixture of three components: dry air, CO_2 gas and water vapour. A separate additional Eulerian phase was used to model condensed water droplets, which were assumed to have the same velocity as the surrounding gas phase. To model the process of condensation, as the temperature fell below the dew point, a source term in the continuity equation for the gas mixture was used to remove the mass of water vapour in excess of the saturation concentration. The same mass, but of liquid water, was added into the dispersed Eulerian water droplet phase via another source term. A third source term in the energy equation was used to account for the release of latent heat. The reverse process of water droplet evaporation was modelled similarly. Independent verification tests were undertaken to ensure that the model was coded correctly. A similar approach to modelling condensation and evaporation was previously tested in the study by Brown and Fletcher (2003).

Sample results from the CFX model in the vicinity of the jet source are shown in Figure 2 for Test Case 3. Gas temperatures were predicted to fall from an initial value of −78ºC to reach a minima of nearly −100ºC at a distance of around 2.5 m downstream from the source. Many of the solid CO_2 particles had sublimated completely by this distance. The maximum distance travelled by the particles was predicted to be around 3.5 m.

4.7 CFD BOUNDARY CONDITIONS

For both OpenFOAM and CFX dispersion models, source conditions for the CO_2 jet were prescribed using values calculated at the position where the jet had expanded to atmospheric pressure, as described in Section 4.3. These conditions included the velocity, the solid CO_2 fraction and the diameter of the source (which was considerably larger than the orifice).

A logarithmic velocity profile was used to model the atmospheric boundary layer in the CFD simulations, using

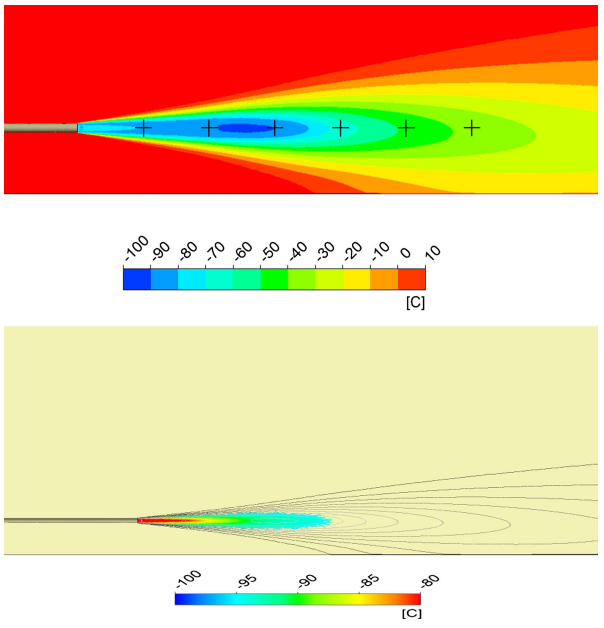

Figure 2. Gas temperature (top) and solid particle temperatures (bottom) predicted by the CFX model for Test Case 3. Cross symbols are spaced at 1 m intervals along the jet axis

the approach described by Richards and Hoxey (1993). To account for the obstructions upstream of the test pad, a ground surface roughness of 0.1 m was used in the logarithmic profile. For the thermal boundary conditions, it was assumed that the boundary layer was neutral. Sensitivity tests showed that the CFD results were unaffected by prescribing either adiabatic or fixed ambient temperature conditions for the ground. Results were also insensitive to the details of the prescribed atmospheric velocity profile. Essentially, in the region of interest for model validation, the flow behaviour was found to be dominated by the jet momentum rather than the atmospheric boundary layer conditions.

The size of the CFD flow domain was set on a case-by-case basis and sensitivity tests were undertaken to ensure that results were unaffected by the location of the domain boundaries. Typically, it extended $100 \times 50 \times 30$ metres in the streamwise $\times$ spanwise $\times$ vertical directions. Sensitivity tests were also undertaken to ensure that the results were reasonably grid-independent. For the CFX results shown here, simulations were performed using approximately 1 million nodes using an unstructured grid, with cells clustered in the jet. Typically there were 600 nodes across the face of the circular source area.

5. RESULTS

In the results shown here, the distance from the jet orifice to the end of the expansion zone has been assumed to be negligible in comparison to the dispersion distances, i.e. the CO_2 source in the dispersion models is located at an axial position of zero.

5.1 DISPERSION FOR UNOBSTRUCTED RELEASES

Three unobstructed steady-state tests at ambient temperature are available from the GL Spadeadam experiments for model validation. The conditions for each of these tests are shown in Table 1. In Test 3 the wind was very well aligned with the jet direction whilst in Tests 5 and 11 the wind direction was slightly less well aligned, with the downstream plume shifting slightly to one side of the initial jet axis. The conditions during the tests were generally either overcast or with a relatively high wind speed. Under such conditions it was considered reasonable to assume neutral stability.

The field temperature measurements on the test pad were found to be relatively steady over the period during which the CO_2 release rate was constant. However, analysis of the CO_2 concentrations measured by the oxygen depletion cells suggested that the devices were adversely affected by the low temperatures in the jet. Rather than average the CO_2 concentrations over the duration of the release, the peak concentration was found to be a better estimate of the true concentration, particularly for those measurements located close to the orifice. Peak values were similar to both the concentrations measured by alternative instruments that did not rely on chemical reactions and to concentrations inferred from the temperature measurements. In the results presented below, two types of experimental concentration results are given – the peak values from the oxygen depletion cells and values inferred from the temperatures.

For the purposes of model validation, the dispersion predictions from the three models can be compared to the

Table 1. Test conditions

	Process Conditions			Ambient Atmospheric Conditions		
Test	Pressure [bara]	Temperature [C]	Hole Size [mm]	Temperature [C]	Relative Humidity [%]	Wind speed [m/s]
3	150	9	12.7	11.2	66	3.9
5	149	17	25.4	9	91	1.3
11	82	−1.5	12.7	3.6	78	2.7

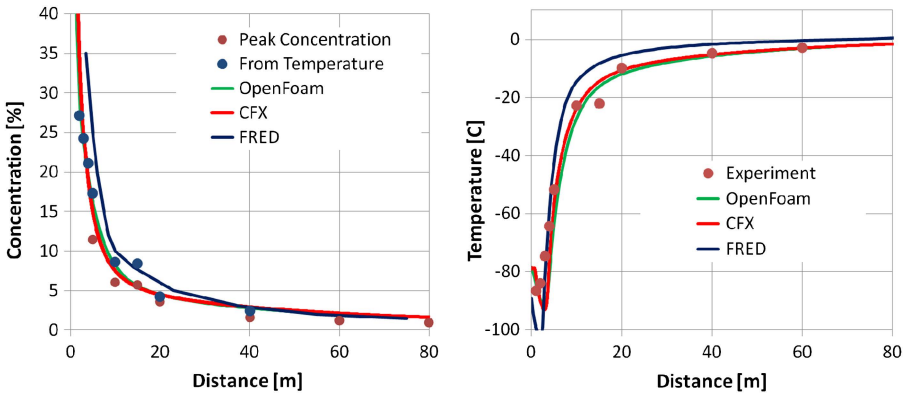

Figure 3. Measured and predicted centreline mole fraction (left) and temperatures (right) for Test 11

experimental data in several ways, such as comparing centreline profiles of concentration or temperature, plume widths at various downstream locations or statistical performance measures (e.g. mean geometric bias). In the present work, centreline values and plume widths are examined. Due to the nature of the experiments, statistical performance measures were found to generally fall well within accepted bounds.

Centreline predictions of the CO_2 concentration and temperature are compared to the measured values at a height of 1 m above grade (i.e. at the release height) for Test 11 in Figure 3. There is a degree of scatter in the experimental concentration values, which were derived from the measured peak concentrations and temperature, as discussed above. However, there is generally good agreement between the experiments and the model predictions for both the temperatures and concentrations. Since FRED treated the solid CO_2 as a liquid, it underpredicted the initial post-flash vapour fraction and underpredicted the temperature in the near-field. The OpenFOAM and CFX results are practically identical to one another, demonstrating that for small particle sizes the flow is close to homogeneous equilibrium.

The CO_2 concentrations on two arcs at 40 m and 60 m at 1 m above ground level are shown in Figure 4 for Test 3. The measured concentrations shown were derived from the temperature measurements and there is therefore a degree of uncertainty in their absolute values. However, the profiles should provide an accurate indication of the plume width. Concentrations inferred from temperature are shown here since the time constant associated with the thermocouples meant that they produced a smoother spanwise plume profile than the raw data from the oxygen depletion cells. The OpenFOAM and CFX results are again similar to one another and show a slightly narrower plume than was measured in the experiments. The FRED model produced slightly better agreement with the data.

Overall, the degree of agreement between the three calculation methods was found to vary from test to test, but in general the predicted plume width at a height of 1 m above the ground was in reasonable agreement in all three experiments with all three codes.

In addition to the concentration and temperature measurements, a large amount of video footage was collected during the experiments. Footage taken from the side of the jet and perpendicular to the jet was found to be useful in order to estimate the initial jet diameter close to the release, where the jet edge was reasonably sharp.

Figure 5 compares the recorded visible jet shape for Test 3 to the OpenFOAM predictions. The edge of the visible jet was digitized at several instants in time from

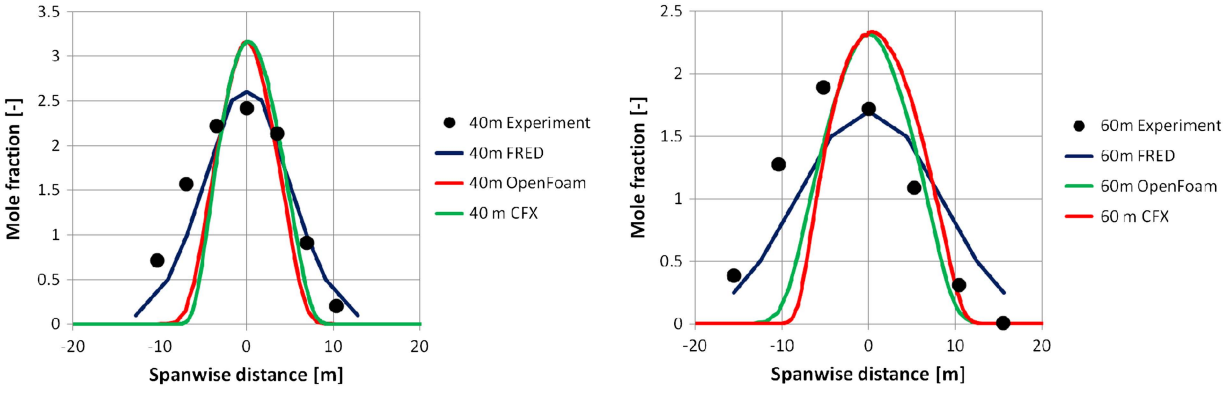

Figure 4. Measured and predicted plume widths at 40 m (left) and 60 m (right) for Test 3

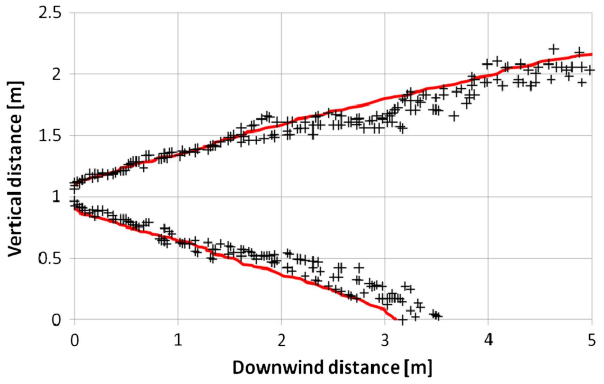

Figure 5. Measured (crosses) and OpenFOAM predictions (line) of plume size in the near field

video footage of a side-on view of the jet, with the results shown as black crosses in Figure 5. Superimposed onto this is the predicted plume width from OpenFOAM. The concentration which best corresponded to the visible jet is not known, but contours have been plotted at a concentration of 1% CO_2 by volume. A contour at a value of 0.1% is only slightly wider, so it is expected that this will give a reasonable indication of the jet edge. The agreement between the model predictions and the measurements is reasonable. The FRED and CFX codes gave comparable results.

5.2 DISPERSION FOR ENCLOSED RELEASES

Some progress has been made in modelling the releases into an enclosure using CFD. It is not possible to simulate this type of release with integral codes such FRED except in a very approximate way. Figure 6 shows the real geometry used in the experiments (shown here by the computer-aided design drawings for the steel fabrication) and the simplified CFD geometry.

The enclosed tests were carried out primarily to study effects such as solid CO_2 deposition within the enclosure, rather than to examine the far-field dispersion. Unfortunately, there were therefore no measurements of temperature or concentration outside of the enclosure. The measurements within the enclosure are also of limited use from a validation perspective – there were several temperature measurement locations but only a single concentration measurement. The temperature measurements were made far inside the enclosure and they all recorded similar temperatures of around -84°C. The OpenFOAM and CFX results agreed well with these measurements. The results from CFX are shown in Figure 7.

The single concentration measurement was located in the lower corner of the enclosure at the enclosed end, and recorded a concentration of around 60% CO_2 by volume. Since the temperature was below -78ºC this implies that there were solids present. The OpenFOAM model predicted a concentration of around 52% at this location while the CFX model gave a value of around 57%. Both of these

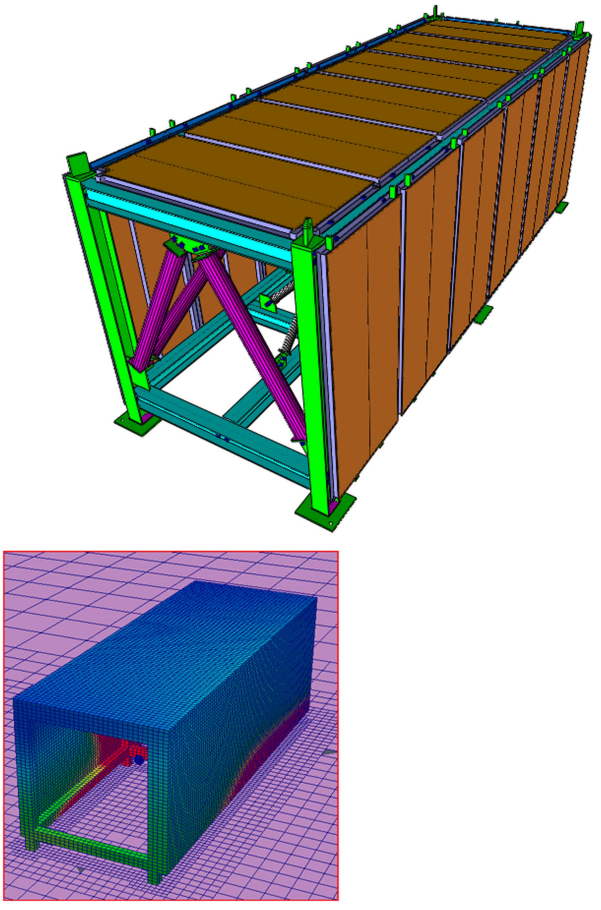

Figure 6. Real enclosure geometry and CFD geometry for the enclosure

values are considered to be in reasonable agreement with experiment.

Although it is not possible to compare the CFD results to measurements outside of the enclosure it is possible to

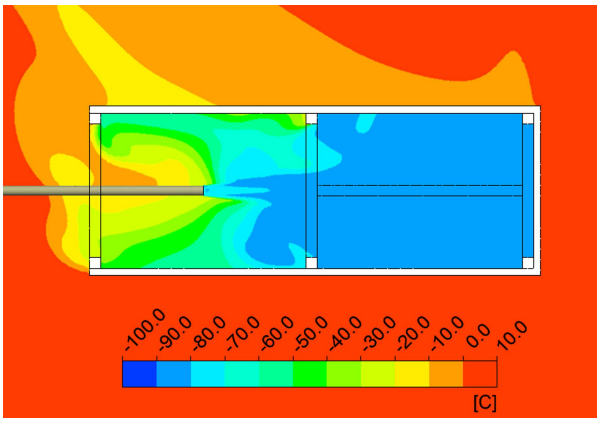

Figure 7. CFD predictions of temperatures on a horizontal plane through the jet in the enclosure

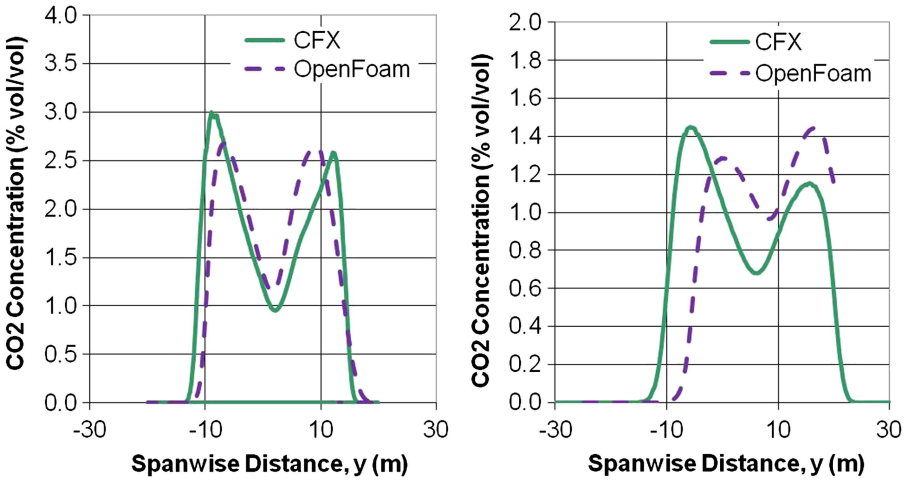

Figure 8. Predicted concentrations on arcs at 20 m (left) and 40 m (right) for enclosure experiment

compare the models to each other. Figure 8 shows the concentrations plotted on arcs at 20 m and 40 m from the release location, at the release height for the enclosure experiment. The agreement between the two models is reasonable, considering that they were constructed completely independently and they employed different sub-models for the solid CO_2 particles.

6. CONCLUSIONS

Three different models have been used to simulate releases of liquid CO_2: FRED, OpenFOAM and CFX. All three models used mass release rates that were calculated using the Bernoulli equation, which was found to provide reasonable predictions of the flow rate for the sub-cooled liquid CO_2 releases considered here.

For the free releases studied, all three models provided generally good predictions of the concentrations along the centreline of the plume. Plume widths were slightly better predicted by FRED than the two CFD models. This may be due to the turbulence models employed in the CFD codes. At a distance of a few metres downstream from the nozzle, the jet became attached to the ground and the flow exhibited behaviour similar to a wall jet. The standard $k-\varepsilon$ turbulence model used by CFX and OpenFOAM is known to have weaknesses in predicting the spreading rate in this type of flow (Craft and Launder, 2001). A more appropriate model could potentially be applied to improve upon this, but it is questionable whether the effort is justified in the context of hazard analysis.

The thermodynamics model employed by FRED did not simulate solid CO_2 particles, but instead extrapolated the liquid-vapour saturation line down to atmospheric pressure. This led to the post-flash vapour fraction being too low and the temperatures being underpredicted in the near-field of the jet. However, this appeared to have a limited effect on the concentration profiles, and even the temperature profiles a few metres downstream were in reasonable agreement with the measurements. Hence it is concluded, for the scale of releases considered here, that FRED performs adequately for the purpose for which it is intended, which is providing hazard distances from free releases.

The CFX model used a particle-tracking approach for the solid CO_2 particles with an initial diameter of 5 μm, whilst the OpenFOAM model assumed homogeneous equilibrium between the particles and the surrounding vapour. The results from the two models were found to be remarkably similar, especially considering that CFD models are known to be sensitive to user inputs and the two models in this case were set up independently by different authors in different organisations. The good agreement between the model predictions and the experiments suggest that it is reasonable to assume a small initial CO_2 particle size, for the scale of releases considered here. Furthermore, the homogenous equilibrium assumption appears to provide an adequate description of the solid CO_2 transport in these cases. For larger-scale releases, such as pipeline full-bore ruptures or catastrophic vessel failures, the size of the CO_2 particles remains uncertain. The effect of larger particles could potentially be examined in the future using the CFX model tested here.

7. DISCLAIMER

The contribution made to this paper by Simon Gant (HSL) and Mike Bilio (HSE) was funded by the Health and Safety Executive (HSE). The contents, including any opinions and/or conclusions expressed, are those of the authors alone and do not necessarily reflect HSE policy.

REFERENCES

ANSYS Inc., 2010, ANSYS CFX-Solver Theory Guide, Release 13.0.

Betteridge, S. and Roy, S., 2010, Shell FRED Technical Guide, Issue 6.0.

Brown, G.J. and Fletcher, D.F., 2003, CFD prediction of odour dispersion and plume visibility for alumina refinery calciner

stacks, 3rd Int. Conf. on CFD in the Minerals and Process Industries, CSIRO, Melbourne, Australia.

Craft, T.J. and Launder, B.E., 2001, On the spreading mechanism of the three-dimensional turbulent wall jet, J. Fluid Mech., vol. 435, pp. 305–326.

Dixon, C. and Hasson, M., 2007, Calculating the release and dispersion of gaseous, liquid and supercritical CO_2, IMechE Seminar on Pressure Release, Fires and Explosions, London.

Dixon, C., Heynes, O. and Hasson, M., 2009, Assessing the hazards associated with release and dispersion of liquid carbon dioxide on offshore platforms, Paper 1651, 8th World Congress of Chemical Engineering, Montreal.

Fauske, H.K. and Epstein, M., 1988, Source term considerations in connection with chemical accidents and vapour cloud modeling, J. Loss Prev. Proc. Ind., vol. 1, pp. 75–83.

Gant, S.E. and Kelsey, A., 2012, Accounting for concentration fluctuations in gaseous releases of carbon dioxide, J. Loss Prev. Proc. Ind., vol. 25, pp. 52–59.

Gosman, A.D. and Ioannides, E., 1981, Aspects of computer simulation of liquid fuelled combustors, AIAA Paper 81–0323, American Institute of Aeronautics and Astronautics.

Harper, P., 2010, The inclusion of CO_2 as a hazardous substance in the Seveso Directive, HSE paper to EC Review of the Seveso II Directive, Health and Safety Executive, Bootle, UK.

Harper, M., 2005, DISC Theory Document, DNV Software.

Hill, T.A., Fackrell, J.E., Dubal, M.R. and Stiff, S.M., 2011, Understanding the consequences of CO_2 leakage downstream of the capture plant, Energy Procedia, vol. 4, pp. 2230–2237 (also published in Int. Conf. On Greenhouse Gas Technologies, GHGT-10, September 2010).

Hulsbosch-Dam, C.E.C., Spruijt, M.P.N., Necci, A. and Cozzani, V., 2012, Assessment of particle size distribution in CO_2 accidental releases, J. Loss Prev. Proc. Ind., vol. 25, pp. 254–262.

Mazzoldi, A., Hill, T. and Colls, J.J., 2011, Assessing the risk for CO_2 transportation within CCS projects, CFD modelling, Int. J. Greenhouse Gas Control, vol. 5, pp. 816–825.

Mazzoldi, A., Hill, T. and Colls, J.J., 2008a, CFD and Gaussian atmospheric dispersion models: A comparison for leak from carbon dioxide transportation and storage facilities, Atmos. Environ., vol. 42, pp. 8046–8054.

Mazzoldi, A., Hill, T. and Colls, J.J., 2008b, CO_2 transportation for carbon capture and storage: Sublimation of carbon dioxide from a dry ice bank, Int. J. Greenhouse Gas Control, vol. 2, pp. 210–218.

Post, L., 1994, HGSYSTEM Technical Reference Manual, HGSYSTEM version 3.0.

McGillivray, A. and Wilday, J., 2009, Comparison of risks from carbon dioxide and natural gas pipelines, HSE Research Report RR749, Health and Safety Executive, Sudbury: HSE Books (http://www.hse.gov.uk/research/rrpdf/rr749.pdf).

Ranz, W.E. and Marshall, W.R., Evaporation from drops, 1952, Chem. Eng. Prog., vol. 48, pp. 141–173.

Richards, P.J. and Hoxey, R.P., 1993, Appropriate boundary conditions for computational wind engineering models using the $k-\varepsilon$ turbulence model, J. Wind Eng. Indust. Aero., vol. 46/47, pp. 145–153.

Schiller, L. and Naumann, A., 1933, Uber die grundlegenden berechungen bei der schwerkraftaufbereitung, Vereines Deutscher Ingenieure, vol.77, pp. 318–320.

Shuter, D., Bilio, M., Wilday, J., Murray, L. and Whitbread, R., 2010, Safety issues and research priorities for CCS systems and infrastructure, Int. Conf. On Greenhouse Gas Technologies GHGT-10.

Webber, D.M., 2011, Generalising two-phase homogeneous equilibrium pipeline and jet models to the case of carbon dioxide, J. Loss Prev. Proc. Ind., vol. 24, pp. 356–360.

Witlox, H.W.M., Harper, M. and Oke, A., 2009, Modelling of discharge and atmospheric dispersion for carbon dioxide releases, J. Loss Prev. Proc. Ind., vol. 22, pp. 795–802.

Witlox, H. W. M., Stene, J., Harper, M. and Nilsen, S. H., 2011, Modelling of discharge and atmospheric dispersion for carbon dioxide releases including sensitivity analysis for wide range of scenarios, Energy Procedia, vol. 4, pp. 2253–2260.